ELSEVIER

Polymer 44 (2003) 2493–2502

polymer

www.elsevier.com/locate/polymer

On the origin of strain hardening in glassy polymers

H.G.H. van Melick, L.E. Govaert*, H.E.H. Meijer

Dutch Polymer Institute (DPI), Section Materials Technology (MaTe), Eindhoven University of Technology, P.O. Box 513, NL-5600MB Eindhoven, The Netherlands

Abstract

The influence of network density on the strain hardening behaviour of amorphous polymers is studied. The network density of polystyrene is altered by blending with poly(2,6-dimethyl-1,4-phenylene-oxide) and by cross-linking during polymerisation. The network density is derived from the rubber-plateau modulus determined by dynamic mechanical thermal analysis. Subsequently uniaxial compression tests are performed to obtain the intrinsic deformation behaviour and, in particular, the strain hardening modulus. At room temperature, the strain hardening modulus proves to be proportional to the network density, irrespective of the nature of the network, i.e. physical entanglements or chemical cross-links. With increasing temperature, the strain hardening modulus is observed to decrease. This decrease appears to be related to the influence of thermal mobility of the chains, determined by the distance to the glass-transition temperature ($T - T_g$).

Keywords: Strain hardening; Network density; Glassy polymers

1. Introduction

In principle all amorphous polymers are intrinsically tough, provided that their molecular weight is sufficiently high (typically eight times the molecular weight between entanglements) to form a sufficiently strong entangled polymer network. However, under certain loading conditions the macroscopic response of these materials to deformation appears to be quite brittle, see Fig. 1a. Polystyrene (PS) and polymethylmethacrylate (PMMA) are considered as such materials which fracture at a few percent of strain under most loading conditions. In polystyrene crack-like defects, so-called crazes, appear in a tensile bar already in the apparent elastic region. With increasing load, the crazes, which are bridged by fibrils, open up and macroscopic fracture occurs upon the failure of these fibrils. That polystyrene is, though, intrinsically ductile can be witnessed from the fact that these fibrils consist of highly stretched material with draw ratios close to the maximum network draw ratio [1,2]. Polycarbonate (PC), on the other hand, is generally considered a ductile material, although it does suffer notch-brittleness. During tensile deformation, a stable neck is formed shortly after yielding. With ongoing strain, the neck grows until ductile fracture occurs at approximately 100% macroscopic strain.

The intrinsic deformation behaviour can be determined in a test where localisation phenomena like necking and crazing are absent. Two examples are a video controlled tensile test [3] and a uniaxial compression test [4,5]. The intrinsic stress–strain curve shows an initial (visco-) elastic region followed by yielding, intrinsic strain softening and strain hardening. Fig. 1b shows that polystyrene, polycarbonate and polymethylmethacrylate exhibit remarkably similar intrinsic behaviour in compression. The initial elastic moduli equal approximately 3 GPa, the yield stresses range from 60 to 120 MPa and depend on strain rate and temperature. The main differences between these materials are found in their post-yield behaviour: (a) the drop in true stress after yielding (intrinsic strain softening or so-called 'yield-drop') and (b) the slope of strain hardening at large strains. This post-yield behaviour plays a key role in the macroscopic deformation behaviour in tension and determines whether a material is brittle or ductile.

Localisation of strain is induced by intrinsic strain softening and the evolution of this localised plastic zone depends on the stabilising effect of the strain hardening [6]. In polystyrene, the substantial strain softening causes severe localisation of plastic strain, which can not be stabilised sufficiently due to the low value of strain hardening modulus. With ongoing deformation, localisation grows to extremes, resulting in void nucleation, craze formation and catastrophic failure. Polycarbonate, on the other hand, has limited strain softening only; the localisation induced is

* Corresponding author. Tel.: +31-40-2472838; fax: +31-40-2447355.
E-mail address: l.e.govaert@tue.nl (L.E. Govaert).

0032-3861/03/$ - see front matter © 2003 Elsevier Science Ltd. All rights reserved.
doi:10.1016/S0032-3861(03)00112-5

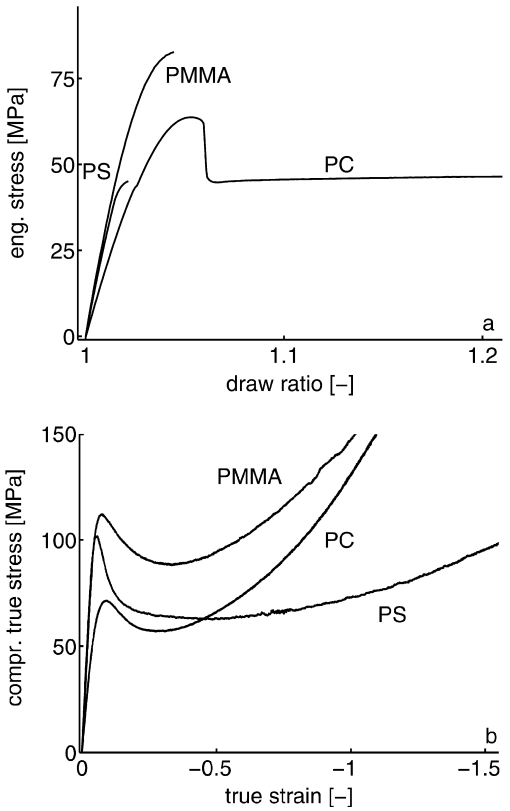

Fig. 1. Deformation behaviour of three well known glassy polymers in tension (a) and compression (b).

therefore moderate and can easily be stabilised by the stronger strain hardening. Polymethylmethacrylate has intermediate properties which leaves it on the edge between brittle and ductile.

The dominant influence of *strain softening* is convincingly demonstrated by the effects of thermal and mechanical histories on macroscopic deformation behaviour. For instance, a quenched specimen exhibits less softening than a slowly cooled specimen in compression tests and, consequently, shows less localised deformation behaviour in tension. Cross and Haward [7] reported uniform deformation for quenched polyvinylchloride (PVC) samples, whereas slowly cooled samples exhibited necking. Various authors showed that by mechanical preconditioning or pre-deformation, the amount of strain softening can be reduced or even eliminated [8–11]. This pre-treatment results in uniform deformation of a polycarbonate tensile bar [10] and can induce ductile deformation behaviour of polystyrene in tension [11]. The crucial role which strain softening plays in the localisation of strain, and hence in the macroscopic deformation behaviour, request a thorough understanding of its molecular background. Despite research efforts [8,12,13], the physical origin of strain softening is not yet fully understood. A fair view point could be that the continuous increase in stress, with a change in slope at the yield point where strain hardening of the polymer network takes over, like it occurs after mechanical rejuvenation or fast quenching, is the natural response of polymers. By the process of physical ageing, the yield stress increases which, on its turn, is accompanied by what is measured as an increasing strain softening. Apparently, further research is necessary long this line (see discussion section of Ref. [14]).

The *strain hardening* behaviour of amorphous and semicrystalline polymers is studied much more extensively. In modelling, effort has been put in numerical simulations of large strain deformation of amorphous, glassy polymers in particular. Most constitutive modelling of strain hardening behaviour is based on the concept of entanglements. Haward and Thackray [15] proposed a constitutive equation in which both a rubber–elastic response and finite extensibility are incorporated. This one-dimensional equation was extended by Boyce et al. [16,17] into a 3-D finite strain formulation, now called the 'BPA-model'. The strain hardening response in this model is represented by a 'three chain' model [18]. The BPA-model was later refined by introducing a more realistic representation of the spatial distribution of molecular chains, resulting in the 'eight chain' model [19] and the 'full chain' model [20].

Haward [21] suggested that polymer coils do not approach a fully stretched condition and hence he proposed a neo-Hookean (Gaussian) relation. Studies of G'Sell [22] and Haward [21,23] showed that for various semi-crystalline polymers this relation describes strain hardening behaviour very well. Tervoort and Govaert [24] investigated this behaviour during uniform deformation of 'pre-conditioned' polycarbonate tensile bars. By mechanical preconditioning, in this case torqueing of cylindrical tensile bars to and fro over 720°, strain softening is eliminated and localisation of strain and necking inhibited. In tensile the strain hardening behaviour was well described by a neo-Hookean relation up to very high draw ratios ($\lambda = 3$). Subsequently, the authors incorporated a neo-Hookean description of the strain hardening behaviour in a Leonov model [25], consisting of a linear compressible spring and an Eyring dashpot [26]. This so-called compressible Leonov model was further extended by Govaert et al. [10] by incorporating intrinsic strain softening. Through finite element simulations of a necking polycarbonate specimen, they showed that limited extensibility is not a prerequisite for stable neck-growth and that this can be simulated perfectly by a neo-Hookean relation.

In all models referred to above, strain hardening is modelled as a rubber–elastic spring, whether or not with finite extensibility, which suggests that the entangled polymer network is involved. The physical relevance of this approach is demonstrated by the complete reversibility of plastic deformation when deformed polymers are brought above their glass transition temperature [27–30].

On the other hand, some data conflict with this entropic character. It was shown by Boyce and Haward [31], Arruda [32] and Tervoort [33] that the strain hardening modulus tends to decrease with temperature whereas the modulus of

a true entropic spring would increase. Moreover, it was shown by Haward [15,24] that the strain hardening modulus is orders of magnitude larger than could be expected from the network density determined in the melt.

This paper addresses this apparent contradiction and the role of the polymer network in the strain hardening behaviour. For this reason, the network density of polystyrene is altered by blending with poly(2,6-dimethyl-1,4-phenylene oxide) (PPO) and by cross-linking during bulk polymerisation. The physical and chemical polymer networks are characterised in the rubbery state by dynamic mechanical thermal analysis (DMTA). From the dynamic modulus (E_d) in the rubbery state, the molecular weight between entanglements (M_e) and the network density (ν_e) are derived. In subsequent uniaxial compression tests, the intrinsic deformation behaviour is determined. The slope, at large strains, of the true stress–true strain curves represents the strain hardening modulus (G_R). Combination enables to investigate the relation between the network density and the strain hardening modulus.

Furthermore, the validity of a neo-Hookean description of strain hardening behaviour is investigated by analytical and numerical tools, employing the previously mentioned compressible Leonov model [26]. Finally, the effect of temperature on the strain hardening modulus is investigated by performing uniaxial compression tests at various temperatures.

2. Materials and methods

The materials used were blends of polystyrene (Styron 638, Dow Chemical Company, The Netherlands) and poly(2,6-dimethyl-1,4-phenylene oxide) (PPO 803, General Electric Plastics, The Netherlands), and polystyrene cross-linked during polymerisation. These materials will be referred to as PS/PPO and XPS. Six blends of PS/PPO were compounded by General Electric Plastics, containing respectively 0, 20, 40, 60, 80, and 100% PPO. The granular material was compression moulded, step-wise, into plates of various thicknesses. Apart from pure PPO, for which a temperature of 260 °C was used to prevent degradation, all material were pre-heated in a mould of 160×160 mm^2 at 80 °C above their glass-transition temperature (T_g) for 15 min and subsequently compressed in the mould in 5 steps of increasing force (up to 300 kN) during 5 min. In between these steps, the pressure was released to allow for degassing. Next, the mould was placed into a cold press and cooled to room temperature at a moderate force (100 kN). Rectangular samples used for DMTA were machined from a 1 mm thick plate with final dimensions of $30 \times 4 \times 1$ mm^3. From thick plates ($160 \times 160 \times 9$ mm^3) rectangular bars with a cross-section of 9×9 mm^2 were cut, which were machined into cylindrical samples (∅6 mm × 6 mm) that were used in the uniaxial compression tests. Cross-linked polystyrene was prepared by bulk-polymerisation of styrene (Aldrich Chemical Company, The Netherlands) and various amounts of cross-linking agent (di-(ethyl glycol)-dimethacrylate, DEGDMA; also from Aldrich). Amounts of 0, 2, 3, 4, and 5% DEGDMA were added to styrene in small glass tubes (∅7 mm × 70 mm). Furthermore, small amounts of initiator (*tert*-butyl proxy benzoate, Trigonox-C, Lamers and Plueger, The Netherlands) and chain transfer agent (dodecanethiol-98%, Aldrich) were added to obtain a desired molecular weight. After filling the tubes, the mixture was fluxed with argon gas to remove the oxygen and were sealed off to prevent evaporation of styrene. Next they were placed in a temperature-controlled silicon-oil bath from which the temperature was slowly raised from 85 to 110 °C in 5 steps of 5 °C and one day duration each. This temperature profile was chosen to avoid auto-acceleration at low conversion rates and to enhance mobility during the propagation stage. Afterwards, the materials were post-cured (without cap) at 120 °C (well above T_g) for 2 days to terminate all reactions and remove all remaining unused monomer. Both DMTA and compression samples were machined from these bars.

DMTA was performed on a Rheometrics Scientific MKIII Dynamic Analyser. A temperature sweep (from room temperature to 250 °C) was used during a dynamic test (tensile set-up) at 1 Hz in order to determine the dynamic modulus (E_d) and the tangent of the phase lag ($\tan(\delta)$).

Compression tests were performed on a servo-hydraulic MTS Elastomer Testing System 810. Cylindrical specimens were compressed at a constant logarithmic strain rate of 10^{-2} s^{-1} between two parallel, flat steel plates. The friction between the sample and steel plates was reduced by an empirically optimised method: onto the sample a thin film of PTFE tape (3M 5480, PTFE skived film tape) was applied and the surface between steel and tape was lubricated by a soap–water mixture. During the compression test no bulging or buckling of the sample was observed, indicating that the friction was sufficiently reduced. The relative displacement of the steel plates was recorded by an Instron (2630-111) extensometer. Both displacement and force were recorded by data acquisition at an appropriate sample-frequency (depending on strain rate). This sampling frequency was adjusted in such a way that a least 1000 data points were collected per test. The set-up for the uniaxial compression tests was placed in a temperature chamber with liquid-nitrogen cooling of which the temperature could be accurately controlled ±0.5 °C). The tests were performed at 25, 45, 65, and 85 °C. Approximately 15 min prior to testing the sample was mounted in the set-up to assure thermal equilibrium.

3. Results

3.1. Dynamic mechanical thermal analysis

The DMTA results for PS/PPO and XPS are given in Fig.

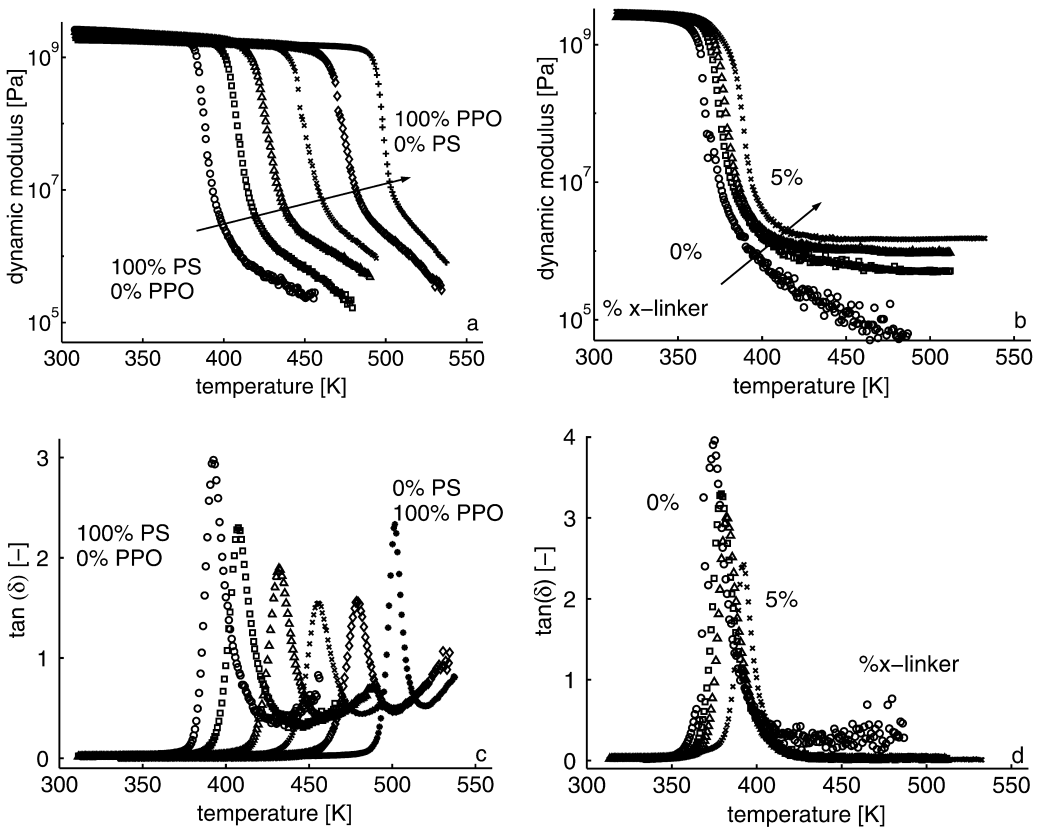

Fig. 2. Results of the DMTA experiments; the dynamic modulus (E_d) and tan(δ) as function of temperature for PS/PPO (a and c) and XPS (b and d).

2. The dynamic modulus (E_d) as function of the temperature is shown in Fig. 2a and b. The PS/PPO blends exhibit the dynamic mechanical response which is characteristic for a thermoplastic material; at room temperature the storage modulus is relatively high, ranging from 2.5 GPa for PPO to 3.0 GPa for PS, and, with increasing temperature, this modulus gradually reduces. At the glass-transition temperature (T_g), a sharp decrease in dynamic modulus is observed, since here the polymer chains obtain full segmental mobility and their state changes from glassy to rubbery.

The phase lag between the input and output signal (tan(δ), see Fig. 2c and d) shows a peak close to T_g, indicating that the contribution of the viscous part to the dynamic response is relatively high in this temperature range. With increasing temperature tan(δ) reduces again and the decay in modulus levels off, indicating that a more elastic region is reached, the so-called rubber plateau. In this rubber–elastic region, the polymer chains have full mobility and the properties are determined by the entangled network. Although the rubber plateau for thermoplastics is not as distinct as for thermosets, the rubber plateau modulus (G_N^0) is defined in this region, as the 'most elastic' dynamic modulus found at the minimum of tan(δ) (see Fig. 2c and Table 1). Upon further heating, the polymer starts to disentangle and the dynamic modulus decays further out of the measurable range. In this temperature range, the onset of a second 'viscous' peak is observed in tan(δ), which indicates that the material becomes liquid-like. The rubber plateau moduli G_N^0 show a continuous increase with PPO content. Values found are similar to values reported in literature [23,34].

The T_gs of the blends increase with increasing PPO fraction, ranging from 378 K for pure PS to 484 K for pure PPO (see Table 1), in good accordance with previously reported data (both DSC and DMTA) on similar blends [34–37]. The fact that only one clear glass-to-rubber transition is observed in the DMTA runs confirms that PS and PPO are miscible on a molecular level and form a compatible mixture.

The response of the in situ polymerised and cross-linked materials is shown in Fig. 2b and d. PS with 0% cross-linking agent behaves similar to the commercial PS,

Table 1
Glass-transition temperatures and rubber plateau moduli for the PS/PPO blends (left) and XPS (right)

% PPO	T_g (K)	T_g (K) Ref. [35]	G_N^0 (MPa) at min. tan(δ)	x-linker (%)	T_g (K)	G_N^0 (Mpa)
0	378	378	0.16	0	362	0.15
20	393	391	0.26	2	368	0.19
40	415	410	0.49	3	372	0.31
60	435	427	0.57	4	377	0.36
80	458	449	0.66	5	383	0.51
100	484	487	0.79			

although some minor differences in modulus and T_g can be caused from differences in molecular weight (distribution) [38]. The cross-linked materials behave like typical thermoset. Above T_g a clear rubber–elastic plateau is reached due to the chemically entangled network. At this plateau the rubber–elastic modulus is defined.

The T_g increases slightly with cross-link density from 362 K for material with 0% cross-linker to 382 K for the material with 5% cross-linker and rubber-plateau modulus increases with cross-link density and their values are given in Table 1.

The rubber(-plateau) moduli, as function of PPO fraction or added amount of cross-linker, are shown in Fig. 3 (solid lines to guide the eye). At low amounts of cross-linker, the rubber modulus does not increase. A reasonable explanation would be that at small amounts of cross-linker the additional cross-links hardly contribute to the rubber modulus and therefore the rubber modulus departs from a plateau (see Fig. 3b).

Moduli can be transformed into network densities using the following equations [39]:

$$G_N^0 = \rho_r \frac{RT}{M_e} \tag{1}$$

where ρ_r is the density of the polymer in the rubbery state, R the molar gas constant and T the absolute temperature. The molecular weight between entanglements M_e, is inversely proportional to the network density (ν_e) according to:

$$\nu_e = \frac{\rho_g N_A}{M_e} \tag{2}$$

where ρ_g is the density of the polymer in the glassy state and N_A the Avogadro number. Zoller and Hoehn [40] performed an extensive investigation of the pressure–volume–temperature properties of PS, PPO and their blends. Their values for the specific volume in the rubbery and glassy state are used here to calculate the network density. For XPS the specific volume of pure PS is used.

Since the variations in density of the PS/PPO blends are small, it is reasonable to anticipate that the relationship between the network density and the rubber-plateau modulus is linear. As a result, the network density also proves to be proportional to the PPO content in the blends (see Fig. 4a). The solid line is the best fit on the experimental data, while the dashed line is derived from the model Prest and Porter [41] used, which states that the molecular weight between entanglements for PS/PPO blends, $M_e(\chi)$ depends solely on the M_e of PS and the fraction (χ) PPO present in blend:

$$M_e(\chi) = \frac{M_e(\mathrm{PS})}{1 + 3.2\chi} \tag{3}$$

Only at high PPO fractions some discrepancy is observed between their model and our experimental data.

In Fig. 4b it is shown that with an increasing amount of

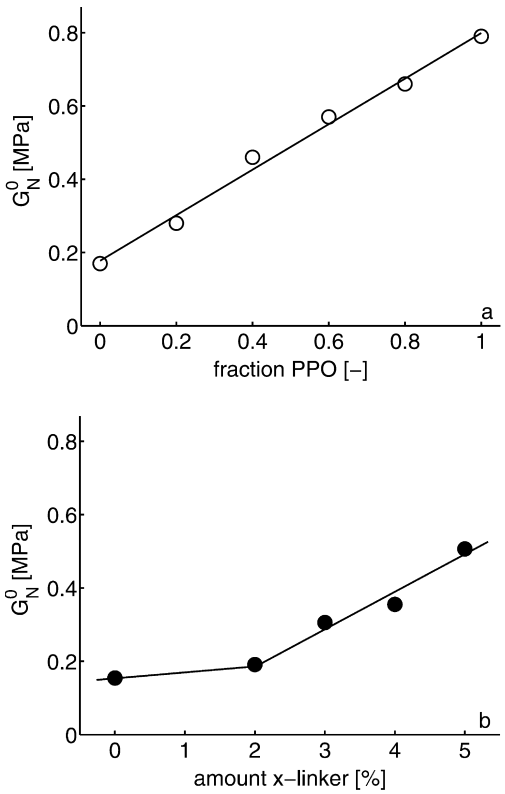

Fig. 3. The rubber(-plateau) moduli as function of fraction PPO (a) and percentage cross-linker (b).

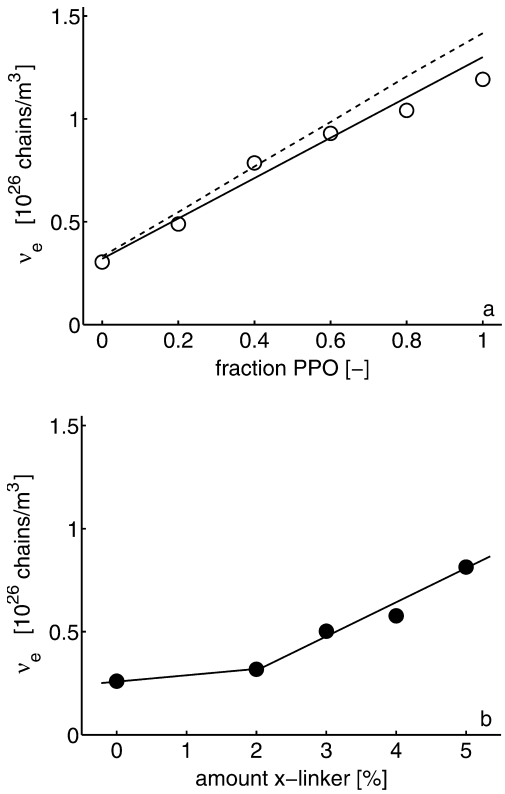

Fig. 4. Network density as function of fraction PPO in PS/PPO (a) and added amount of cross-linker in XPS (b).

cross-linker added during polymerisation, the network density increases. Similar to the results of Fig. 3b, the influence of small amount of cross-linker on the network density is low and therefore it is reasonable to assume that the network density also departs from a plateau, represented by the solid line in Fig. 4b.

3.2. Uniaxial compression tests

The effect of an increased network density on the post-yield behaviour was investigated by uniaxial compression tests. Since localisation phenomena like crazing and necking are absent in such tests, a true stress–true strain curve is obtained, see Fig. 5. From these results, it can be concluded that the post-yield behaviour is strongly influenced by a change in network density. For increasing network density, i.e. increasing PPO fraction or increasing the amount of cross-linker, the strain hardening modulus clearly rises, while the yield stress, which is mainly determined by the secondary interactions between the polymer chains, remains largely unaffected. The fact that strain softening, which is also governed by secondary interactions, decreases with increasing network density must be attributed to the stabilising contribution of the polymer network, that shows a noticeable effect at small strains. Hence, the true stress cannot drop as much as in a looser network.

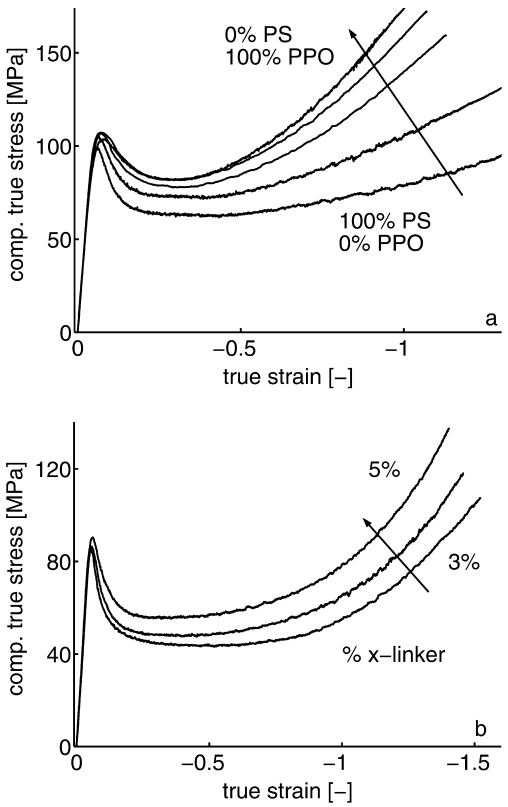

Fig. 5. Compressive behaviour of PS/PPO (a) and XPS (b) at room temperature and at a strain rate of $10^{-2}\,s^{-1}$.

From the uniaxial compression curves at large strains, the strain hardening moduli were determined. From the strain energy function, first proposed by Mooney [42], for rubber–elastic materials, it can be derived that the true stress is proportional to $\lambda^2 - \lambda^{-1}$. If a neo-Hookean description is valid for the strain hardening behaviour of these materials, the true stress should be proportional to this strain measure. In Fig. 6a it is shown that for the PS/PPO blends the true stress is indeed linear in $\lambda^2 - \lambda^{-1}$. The strain hardening modulus is defined as the slope at large strains, which is schematically represented by the dashed line in Fig. 6a. An identical procedure is followed to determine the strain hardening moduli of XPS.

The validity of a neo-Hookean description of the large-strain behaviour of these materials is illustrated by numerical simulations, performed with MARC (MSC Software) employing the compressible Leonov model [10, 26,43] with a neo-Hookean relation representing the large strain behaviour. In Fig. 6b it is shown that the simulations provide a good description of the uniaxial compression tests, indicating that the strain-hardening behaviour can indeed adequately be described by a neo-Hookean relation.

Finally, combining the results of the DMTA experiments and the uniaxial compression tests yields the relation sought between the network density and the strain hardening modulus. In Table 2 the values for the network density and strain hardening modulus of the various materials are given,

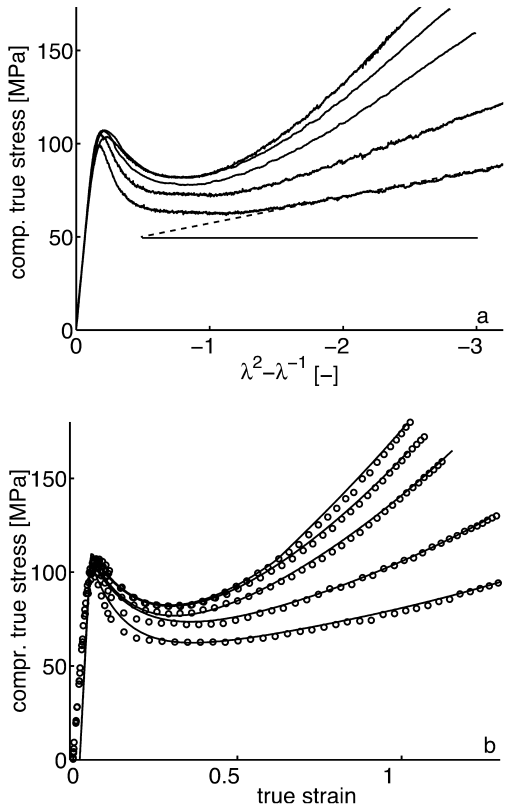

Fig. 6. A neo-Hookean relation can adequately describe the strain hardening behaviour as is shown by analytical (a) and numerical methods (b).

Table 2
Network density, ν_e, and strain hardening moduli, G_R, for all materials

		ν_e (10^{26} chains m^{-3})	G_R (MPa)
PS/PPO	100/0	0.30	13
	80/20	0.49	25
	60/40	0.79	48
	40/60	0.93	58
	20/80	1.04	65
	0/100	1.19	75
XPS	0%	0.26	13
	2%	0.32	23
	3%	0.5	27
	4%	0.58	33
	5%	0.81	45

while in Fig. 7 the strain hardening modulus is plotted versus the network density (the open circles represent the PS/PPO blends, the filled circles XPS). Similar to rubber–elastic behaviour the strain hardening modulus proves to be proportional to the network density, irrespective of the nature of the polymer network, i.e. physical entanglements or chemical cross-links.

So far the experimental and numerical results indicate a neo-Hookean relation to provide an adequate description of the strain hardening behaviour of amorphous polymers. However, as was already shown by several authors [31–33], the strain hardening modulus decreases with temperature. In Fig. 8a the strain hardening modulus of the PS/PPO blends is given as function of temperature. Obviously, the strain hardening moduli are inversely proportional to the temperature (the lines are drawn as a guide to the eye) and this becomes more pronounced at high PPO fractions in the blend.

Representing the strain hardening modulus as function of network density, which is a characteristic of each blend, gives a bundle of straight lines with proportionality constant c, see fig. 8b, according to:

$$G_R = c(T)\nu_e \quad (4)$$

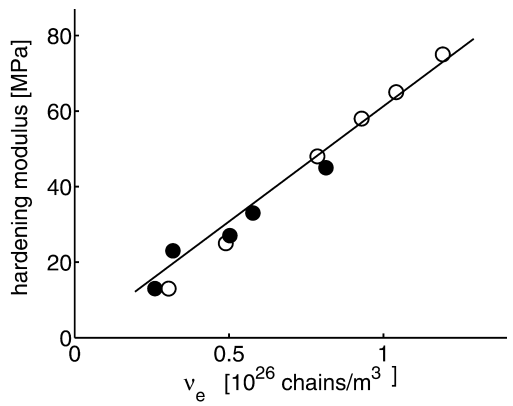

Fig. 7. Strain hardening modulus, G_R, versus the network density, ν_e, for all materials investigated.

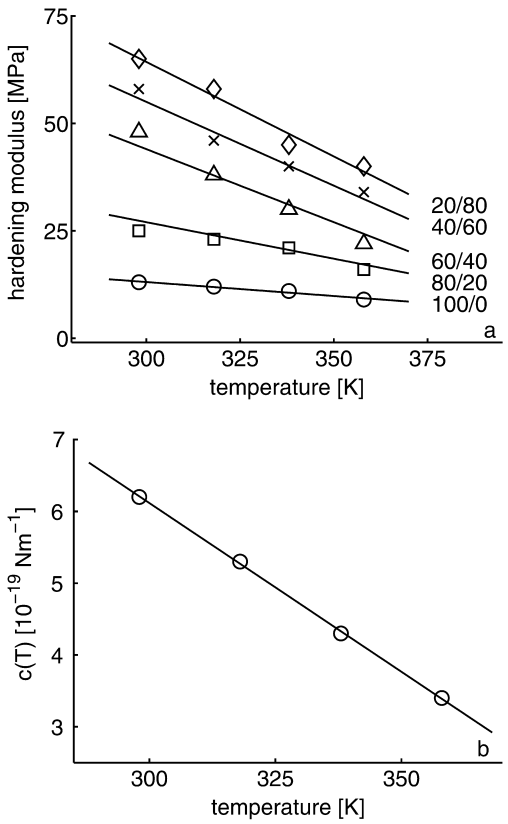

Fig. 8. The strain hardening modulus for the PS/PPO blends (a), and the proportionality constant c (Eq. (4)) (b) as function of temperature.

The nature of the negative temperature dependence of this proportionality constant is discussed in Section 4.

4. Discussion

In case of an entropic spring a proportionality constant equal to ρRT would be expected, and hence an increasing modulus with temperature. This clearly indicates that strain hardening behaviour is not unambiguously of an entropic nature. As can be concluded from Fig. 7, the strain hardening modulus is related, and even proportional, to the rubber-plateau modulus measured in the melt. One could argue that the trend of the increasing strain hardening modulus with increasing PPO content can be fully addressed to the changes in secondary interactions caused by the differences in chemical structure of polystyrene and polyphenylene-oxide. However, the increasing strain hardening modulus with cross-link density proves that the density of the polymer network governs the large strain behaviour. This relationship between the strain hardening modulus and the rubber-plateau modulus seems to suggest that these phenomena have a common (micro-)structural background.

It is well known that in the melt, where the rubber-plateau modulus is determined, polymer chains have full main-chain segmental mobility, which is thermally induced.

The dynamic response, measured in this region, is fully dependent on the molecular network as on this time-scale the contribution of secondary interactions is negligible. The time and temperature-dependent behaviour in this region has been subject to many studies in the past and the validity of the reptation theory is quite well established, see e.g. Ref. [44,45]. The response in this region is governed by entropy elasticity and relaxation, which implies that both time and temperature play an important role.

During plastic deformation in the glassy state, polymer chains also obtain a certain degree of mobility, albeit of different nature: stress-induced instead of temperature-induced main-chain segmental mobility. That this mobility does activate a contribution of the molecular network can be witnessed from the fact that chemical cross-linking does have a significant effect on the strain hardening modulus and that plastic deformation is fully reversible by bringing the polymer above its glass-transition temperature [27–30].

The higher values of the strain hardening modulus, compared to the rubber-plateau modulus, might originate from the difference in nature of the mobility obtained. Although the material is deformed in the glassy state, it is reasonable to assume that under the influence of the applied stress, the polymer molecules only obtain a limited degree of mobility. Several experimental studies showed that mobilisation of chains occurs under influence of stress at the crack tip during crazing and that the model of reptation might be used in certain cases in the glassy state [46–48]. Numerical simulations by Tervoort et al. [49] suggested that yielding in glassy polymers can be regarded as a stress-induced glass-to-rubber transition. A natural assumption would be that the time-scale of the stress-induced main-chain segmental mobility during yielding is equal to the time-scale on which the experiment is performed. It is well known that the time-scale of main-chain segmental mobility in, for instance, a DMTA is influenced by temperature. In the glassy state, far below T_g, the time-scale of main-chain segmental mobility is much longer than the time-scale of the experiment, whereas in the rubbery state, far above T_g, the time-scale of main-chain segmental mobility is much shorter than the time-scale of the experiment. In a way one could regard the stress-induced main-chain segmental mobility during yielding analogous to a DMTA at a temperature at which the time-scale of the thermally-induced main-chain segmental mobility is equal to the excitation frequency, i.e. right at the glass transition temperature. So one could qualify the main chain segmental mobility, induced by yielding, as partial main-chain segmental mobility with a significant contribution of the secondary interactions which are not fully relaxed. Similar to a thermodynamic glass-to-rubber transition, the modulus measured in this region is higher than the rubber-plateau modulus in the melt but still the entangled polymer network does contribute to the response.

Moreover, one could imagine that on top of this stress-induced main-chain segmental mobility a thermally-induced segmental mobility can be superposed. Testing at an elevated temperature could result in a higher overall segmental mobility and therefore lead to a lower strain hardening modulus.

In this respect, a useful representation of the data of Fig. 8a is to compare the strain hardening moduli at ΔT to their respective glass transition temperatures. In this way, a correction is made for the differences in segmental mobility between the different blends. In Fig. 9 the strain hardening moduli are plotted versus measuring temperature minus T_g.

Clearly the strain hardening modulus decreases when the measuring temperature approaches T_g. For high fraction PPO and thus far from T_g the curves from Fig. 8a shift to a apparent master curve. For low fractions of PPO and pure PS and thus close to T_g the curves deviate from the apparent master curve and decrease more rapidly with decreasing network density. In the light of the previous discussion, this can be interpreted by two contributions governing in different parts of the temperature regime. At relative low temperatures, far from T_g the influence of the thermal mobility on the strain hardening modulus is prevalent and no significant contribution of the polymer network is observed. Closer to T_g the influence of thermal mobility diminishes and the polymer network becomes an important parameter in the strain hardening response, as it shows a clear dependence on the density of the network.

5. Conclusions

In this paper the role of the network density on the strain hardening behaviour of amorphous polymers has been investigated. The network density of glassy polystyrene was altered by blending with polyphenylene oxide and by cross-linking. The blends of PS and PPO are fully compatible in all mixing ratios and form a mixture on a molecular scale. This can be witnessed from the fact that in DMTA only one glass transition temperature is observed. From these tests, it was also concluded that the glass transition temperature and the rubber modulus (dynamic modulus determined in the

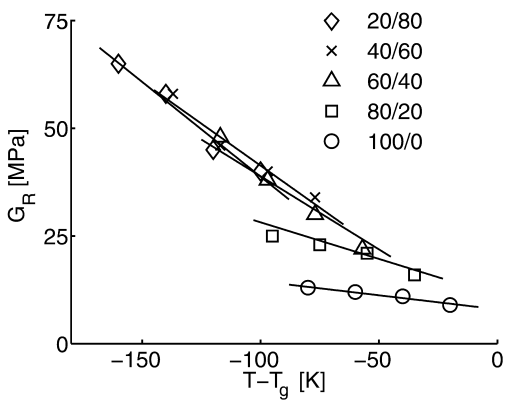

Fig. 9. The strain hardening modulus for the PS/PPO blends as a funtion of $(T - T_g)$.

rubbery state) increase with increasing PPO fraction in the blend. The DMTA experiments of cross-linked polystyrene (XPS) show, besides a slight increase in T_g, an increased rubber-plateau modulus with an increasing amount of added cross-linking agent. From the rubber(-plateau) moduli the network density was derived using equations from the rubber–elastic theory. Experimentally determined network densities correlate well with the model proposed by Prest and Porter [41]. Uniaxial compression tests showed minor changes in the elastic and yield behaviour of the PS/PPO blends; the main differences were found in the strain hardening behaviour. With increasing PPO fraction in PS/PPO and an increasing amount of cross-linker in XPS the strain hardening modulus increases. Numerical and analytical approaches demonstrated that the strain hardening behaviour can be adequately described by a neo-Hookean relation.

Representing the strain hardening modulus as function of the network density, obtained from DMTA experiments, yields the conclusion that the strain hardening modulus is proportional to the network density, irrespective of the nature of the entangled polymer network, i.e. physical entanglements or chemical cross-links.

However, the strain hardening modulus measured in uniaxial compression tests as function of temperature contradicts the similarity with rubber–elastic behaviour. With increasing temperature, the strain hardening modulus decreases whereas for an entropic spring it is expected to rise. It was discussed that after yielding, which can be interpreted as a stress-induced rubbery state, the polymer network is addressed but that relaxation mechanisms might also play an important role. In the temperature dependence of the strain hardening behaviour, relaxation might overrule the entropic character of the polymer network and lead to a decreasing trend. Taking the differences in molecular mobility of the various blends into account, by representing the strain hardening data versus $T - T_g$, supports the suggestion that both the thermal mobility and the entangled polymer network contribute to the strain hardening modulus.

Acknowledgements

The authors wish to acknowledge Theo Tervoort for his valuable contribution to the discussion and the financial support provided by the Dutch Technology Foundation (STW) (Grant EWT.3766).

References

[1] Donald AM, Kramer EJ. Polymer 1982;23(3):457–60.
[2] Donald AM, Kramer EJ, Bubeck RA. J Polym Sci, Polym Phys Ed 1982;20(7):1129–41.
[3] G'Sell C, Hiver JM, Dahouin A, Souahi A. J Mater Sci 1992;27(18):5031–9.
[4] Arruda EM, Boyce MC. Int J Plast 1993;9(6):697–720.
[5] Boyce MC, Arruda EM, Jayachandran R. Polym Engng Sci 1994;34(9):716–25.
[6] Meijer HEH, Govaert LE, Smit RJM. A multi-level finite element method for modeling rubber-toughened amorphous polymers. In: Pearson R, editor. Toughening of plastics. Boston: American Chemical Society; 1990. p. 50–70.
[7] Cross A, Haward RN, Mills NJ. Polymer 1979;20(3):288–94.
[8] G'Sell C. Plastic deformation of glassy polymers: constitutive equations and macromolecular mechanisms. In: McQueen H, editor. Strength of metals and alloys. Oxford: Pergamon Press; 1986. p. 1943–82.
[9] Bauwens JC. J Mater Sci 1978;13(7):1443–8.
[10] Govaert LE, Timmermans PHM, Brekelmans WAM. J Engng Mater Technol 2000;122(2):177–85.
[11] Govaert LE, van Melick HGH, Meijer HEH. Polymer 2001;42(3):1271–4.
[12] Aboulfaraj M, G'Sell C, Mangelinck D, McKenna GB. J Non-Crystalline Solids 1994;172–174:615–21.
[13] Hasan OA, Boyce MC. Poymer 1993;34(24):5085–92.
[14] van Melick HGH, Govaert LE, Raas B, Nauta WJ, Meijer HEH. Kinetics of ageing and re-embrittlement of mechanically rejuvenated polystyrene. Polymer 2003;44(4):1171–9.
[15] Haward RN, Thackray G. Proc R Soc Lond Ser A 1967;302(1471):453–72.
[16] Boyce MC, Parks DM, Argon AS. Mech Mater 1988;7(1):15–33.
[17] Boyce MC, Arruda EM. Polym Engng Sci 1990;30(20):1288–98.
[18] James HM, Guth E. J Chem Phys 1943;11:455–81.
[19] Arruda EM, Boyce MC. J Mech Phys Solids 1993;41(2):389–412.
[20] Wu PD, van der Giessen E. J Mech Phys Solids 1993;41(3):427–56.
[21] Haward RN. J Polym Sci Part B: Polym Phys 1995;33(10):1481–94.
[22] G'Sell C, Boni S, Shrivastava S. J Mater Sci 1983;18(3):903–18.
[23] Haward RN. Macromolecules 1993;26(22):5860–9.
[24] Tervoort TA, Govaert LE. J Rheol 2000;44(6):1263–77.
[25] Leonov AI. Rheol Acta 1976;15:85–98.
[26] Tervoort TA, Smit RJM, Brekelmans WAM, Govaert LE. Mech Time-dependent Mater 1998;1(3):269–91.
[27] Gurevich G, Kobeko P. Rubb Chem Technol 1940;13:904–17.
[28] Haward RN. Trans Faraday Soc 1942;38:394–403.
[29] Hoff EAW. J Appl Chem 1952;2:441–8.
[30] Haward RN, Murphy BM, White EFT. J Polym Sci, Part A-2 1971;9(5):801–14.
[31] Boyce MC, Haward RN. The post-yield deformation of glassy polymers. In: Haward RN, Young RJ, editors. The physics of glassy polymers, 2nd ed. London: Chapman & Hall; 1997. p. 213–93.
[32] Arruda EM. Charaterization of the strain hardening response of amorphous polymers. PhD Thesis, Massachusetts Institute of Technology; 1992.
[33] Tervoort TA. Constitutive modelling of polymer glasses, finite, nonlinear viscoelastic behaviour of polycarbonate. PhD Thesis, Eindhoven University of Technology; 1996.
[34] Wu S. J Polym Sci Part B: Polym Phys 1987;25(12):2511–29.
[35] Creton C, Halary J-L, Monnerie L. Polymer 1998;40(1):199–206.
[36] Cowie JMG, Harris S, Gómez Ribelles JL, Meseguer JM, Romero F, Torregrosa C. Marcomolecules 1999;32(13):4430–8.
[37] Robertson CG, Wilkes GL. Polymer 2000;41(26):9191–204.
[38] Kumar A, Gupta RK. Fundamentals of polymers. London: McGraw-Hill; 1998.
[39] Treloar LRG. The physics of rubber elasticity, 3rd ed. Oxford: Clarendon Press; 1975.
[40] Zoller P, Hoehn HH. J Polym Sci, Polym Phys Ed 1982;20(8):1385–97.
[41] Prest jr WM, Porter RS. J Polym Sci, Part A2: Polym Phys 1972;10(9):1639–55.
[42] Mooney M. J Appl Phys 1940;11:582.

[43] van der Aa MAH, Schreurs PJG, Baaijens FPT. Mech Mater 2001;33: 555–72.
[44] de Gennes PG. J Chem Phys 1971;55(2):572–9.
[45] Doi M, Edwards SF. The theory of polymer dynamics. Oxford: Oxford University Press; 1986.
[46] Prentice P. Polymer 1983;24(3):344–50.
[47] Evans KE. J Polym Sci, Part B: Polym Phys 1987;25(2):353–68.
[48] McLeish TCB, Plummer CJG, Donald AM. Polymer 1989;30(9): 1651–5.
[49] Tervoort TA, Klompen ETJ, Govaert LE. J Rheol 1996;40(5): 779–97.